*Seo et al.:*

# Evaluation of an *In Vitro* Three-dimensional HepaRG Spheroid Model for Genotoxicity Testing using the High-throughput CometChip Platform

## Supplementary Data

**Tab. S1: Comparison of the benchmark dose ($BMD_{50}$) and potency ranking between 2D and 3D HepaRG cultures**[a]

| Chemical | 2D | | | 3D | | |
|---|---|---|---|---|---|---|
| | $BMD_{50}$ (µM) | $BMDL_{50}$–$BMDU_{50}$ (µM) | U/L | $BMD_{50}$ (µM) | $BMDL_{50}$–$BMDU_{50}$ (µM) | U/L |
| $CdCl_2$ | - | - | - | 0.6 (1) [b] | 0.4–1.1 | 3.1 |
| 4-NQO | 2.3 (1) | 1.4–4.2 | 3.1 | 0.8 (2) | 0.5–1.1 | 2.1 |
| DMNA | 879.3 (10) | 535–1340 | 2.5 | 2.4 (3) | 1.3–4.5 | 3.6 |
| Cisplatin | 45.2 (5) | 23.7–105 | 4.4 | 5.5 (4) | 3–9.6 | 3.2 |
| MMS | 5.2 (2) | 2.5–9.2 | 3.7 | 7.7 (5) | 4.5–12.9 | 2.9 |
| B[*a*]P | 22.8 (4) | 14.7–34.8 | 2.4 | 12.1 (6) | 6.9–21.1 | 3.1 |
| Etoposide | 11.2 (3) | 5–27.9 | 5.6 | 18.3 (7) | 10–35.1 | 3.5 |
| IQ | - | - | - | 69.3 (8) | 41.4–121.0 | 2.9 |
| PhIP | - | - | - | 93.5 (9) | 52.7–179 | 3.4 |
| DMBA | 568 (7) | 352–967 | 2.7 | 163.6 (10) | 93.3–288 | 3.1 |
| ENU | 686.5 (9) | 453–1000 | 2.2 | 355.3 (11) | 202–629 | 3.1 |
| Acrylamide | 379.1 (6) | 193–754 | 3.9 | 385.3 (12) | 221–638 | 2.9 |
| CPA | 9011 (12) | 4710–21200 | 4.5 | 427.3 (13) | 251–698 | 2.8 |
| 3-MCPD | 3386 (11) | 1710–8300 | 4.9 | 1064 (14) | 619–1730 | 2.9 |
| 2,4-DAT | - | - | - | 1270 (15) | 779–2060 | 2.6 |
| Ethyl acrylate | 614 (8) | 340–1130 | 3.3 | - | - | - |

[a] BMDs for the CometChip data were calculated using PROASTweb. [b] Potency ranking. $CdCl_2$, cadmium chloride; 4-NQO, 4-nitroquinoline 1-oxide; DMNA, dimethylnitrosamine; MMS, methyl methanesulfonate; B[a]P, benzo[a]pyrene; IQ, 2-amino-3-methylimidazo[4,5-f]quinoline; PhIP, 2-amino-1-methyl-6-phenylimidazo[4,5-b]pyridine; DMBA, 7,12-dimethylbenzanthracene; ENU, N-ethyl-N-nitrosourea; CPA, cyclophosphamide; 3-MCPD, 3-chloro-1,2-propanediol; 2,4-DAT, 2,4-diaminotoluene.

doi:10.14573/altex.2201121s

**Tab. S2: Characterization of primary human hepatocytes of each donor (provided by the supplier)**

| Characterization | | Lot# HH1085 | Lot# HH1090 | Lot# HH1054 |
|---|---|---|---|---|
| Donor Demographics | Gender | Female | Female | Male |
| | Age | 77 | 4 | 23 |
| | Race | Hispanic | Hispanic | Caucasian |
| | Cause of death | CVA 2nd to ICH | Gastric perforation | Head trauma |
| | BMI | 30.3 | 18.2 | 25.3 |
| | Smoking | No | No | No |
| | Alcohol | No | No | Yes |
| | Substance abuse | No | No | No |
| | Medical history | Asthma, HTN | Chromosome abnormality | NA |
| | Infectious diseases | HBV-, HCV-, HIV-, CMV+, EBV (IgG)+ | HBV-, HCV-, HIV-, CMV-, EBV (IgG)+ | HBV-, HCV-, HIV-, CMV+ |
| Classification | Plateability | Plateable | Plateable | Plateable |
| | Number of days plateable | Over 5 days | 3 days | 5 days |
| | Confluency | 100% | 100% | 70% |
| | P450 Inducibility | Yes | ND | Yes |
| | Transporter activity | CDFDA efflux qualified pravastatin uptake qualified | ND | No |
| Post-thaw Viability | Viability | 94% | 91% | 95% |

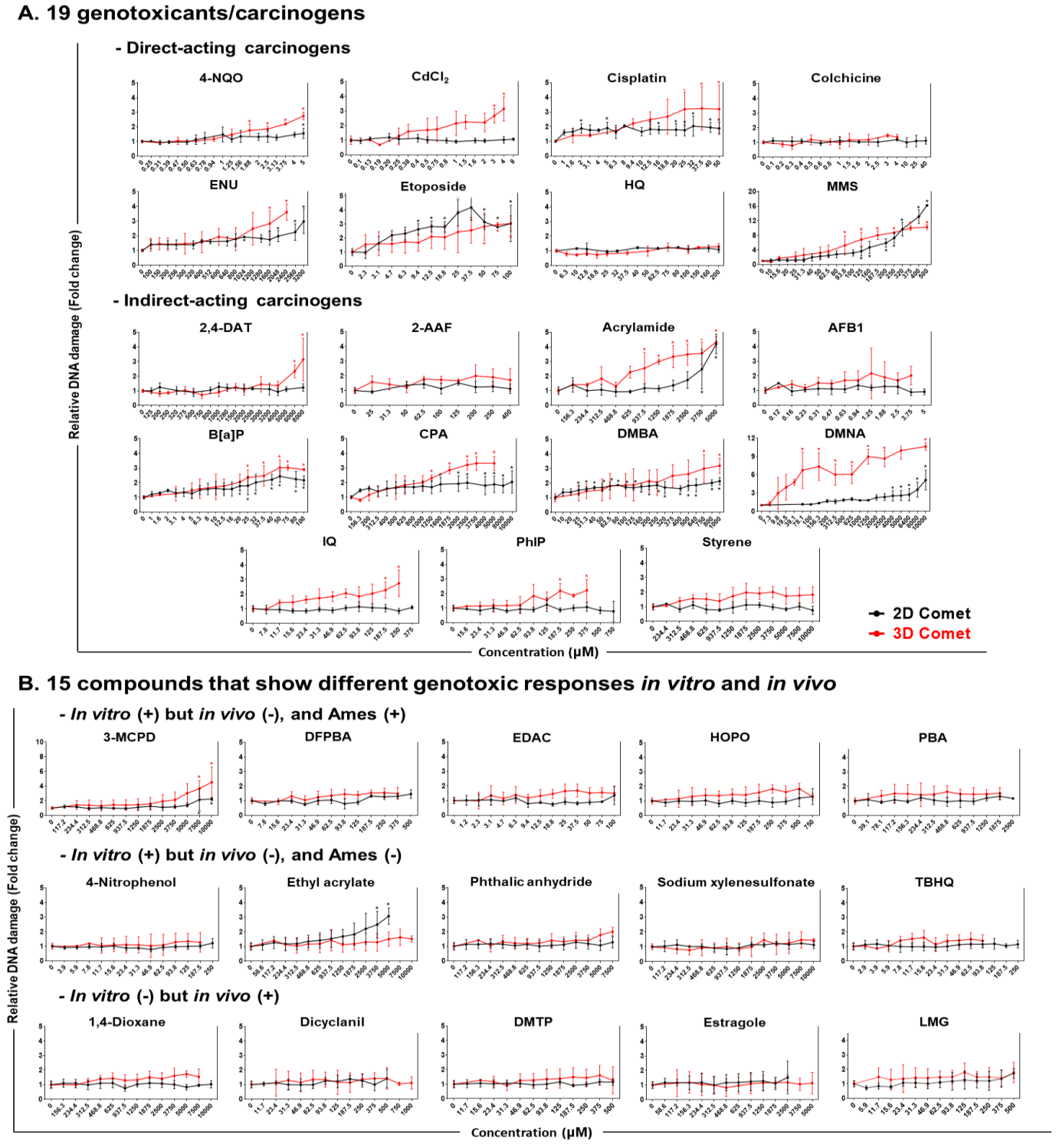


**Fig. S1: The relative ratios of DNA damage of 8 direct-acting and 11 indirect-acting genotoxicants/carcinogens (A) and 15 compounds that show different genotoxic responses *in vitro* and *in vivo* (B) in 2D and 3D HepaRG cultures**
Following 24-h treatment, the relative ratios of DNA damage (fold change) were compared to their respective controls in 2D and 3D HepaRG cultures (black and red lines, respectively). The data are expressed as the mean ± SD (n ≥ 3). Significant differences were determined by one-way ANOVA followed by Dunnett's test (*$p$ < 0.05 vs. vehicle control).

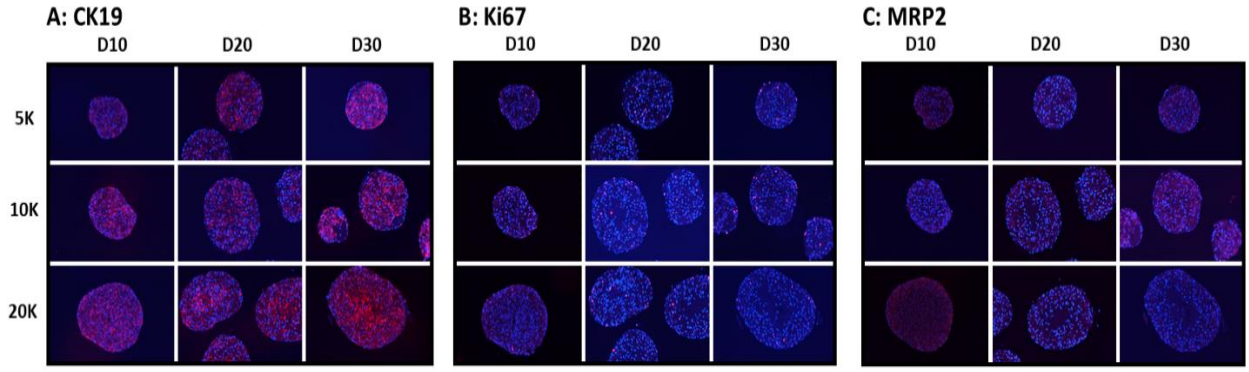


**Fig. S2: Immunofluorescent staining with CK19 (A), Ki67 (B), and MRP2 (C) in 5K, 10K, and 20K spheroids at Days 10, 20, and 30**
CK19, cytokeratin 19; MRP2, multidrug resistance-associated protein 2

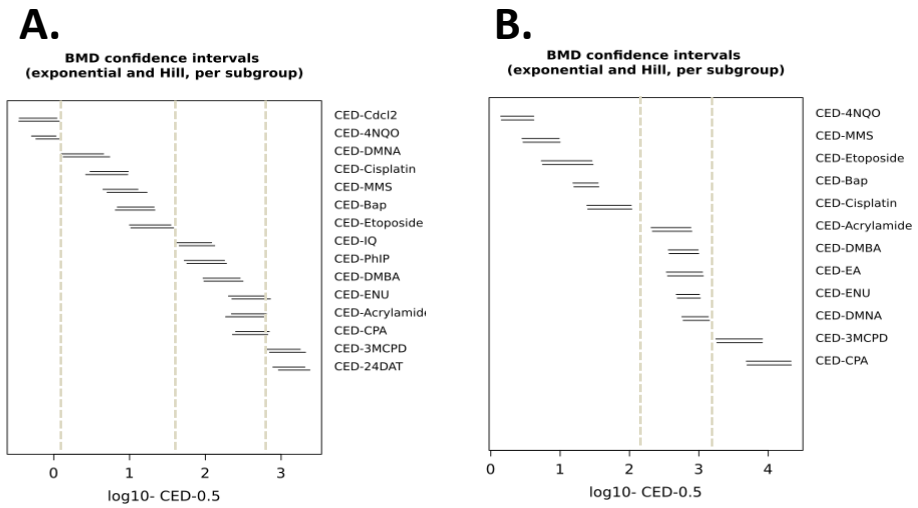


**Fig. S3: Covariate benchmark dose analysis (BMD) of DNA damage with their 90% confidence intervals in 3D (A) and 2D (B) HepaRG cultures**
Part of DNA damage concentration-response data in 2D HepaRG cells were obtained from our previous study (Seo et al. 2019). $BMD_{50}$ and their 90% confidence limits (BMDL and BMDU) were calculated from 2D and 3D CometChip data using exponential (upper line) and Hill (lower line) models of PROAST. The lower and upper limits derived from the BMD estimates were used to differentiate between responses based on non-overlapping confidence intervals.